Phys. Status Solidi C **7**, No. 2, 362–365 (2010) / **DOI** 10.1002/pssc.200982473

physica status solidi c
www.pss-c.com
current topics in solid state physics

Do we know the band gap of lithium niobate?

C. Thierfelder[*], **S. Sanna, Arno Schindlmayr, and W. G. Schmidt**

Department Physik, Universität Paderborn, 33095 Paderborn, Germany

Received 6 July 2009, revised 24 September 2009, accepted 6 October 2009
Published online 10 December 2009

PACS 71.15.Qe, 71.20.Ps, 71.45.Gm

[*] Corresponding author: e-mail c.thierfelder@uni-paderborn.de, Phone: +49-5251-602339, Fax: +49-5251-603435

Given the vast range of lithium niobate ($LiNbO_3$) applications, the knowledge about its electronic and optical properties is surprisingly limited. The direct band gap of 3.7 eV for the ferroelectric phase – frequently cited in the literature – is concluded from optical experiments [1]. Recent theoretical investigations [2] show that the electronic band-structure and optical properties are very sensitive to quasiparticle and electron-hole attraction effects, which were included using the *GW* approximation for the electron self-energy and the Bethe-Salpeter equation respectively, both based on a model screening function. The calculated fundamental gap was found to be at least 1 eV larger than the experimental value. To resolve this discrepancy we performed *first-principles GW* calculations for lithium niobate using the full-potential linearized augmented plane-wave (FLAPW) method [3]. Thereby we use the parameter-free random phase approximation for a realistic description of the nonlocal and energy-dependent screening. This leads to a band gap of about 4.7 (4.2) eV for ferro(para)-electric lithium niobate.

1 Introduction Lithium niobate ($LiNbO_3$, LN) is due to its distinguished photo-refractive, electro-optic, and nonlinear optical properties exploited in a number of devices such as Pockels cells, optical parametric oscillators, Q-switching devices for lasers and optical switches for gigahertz frequencies. LN occurs in two phases of trigonal symmetry with ten atoms per unit cell, see Fig. 1. The ground-state is ferroelectric with space group $R3c$. The high-symmetric paraelectric phase with space group $R\bar{3}c$ is stable above 1480 K. Given the vast range of LN applications, our knowledge about its electronic and optical properties is surprisingly limited. For example, we are not aware of a measured band structure. The direct band gap of 3.78 eV for the ferroelectric phase – frequently cited in the literature – is actually concluded from optical experiments [4]. Therefore it is affected by electron-hole attraction effects which may reduce the size of the actual band gap, i.e., the difference between the ionization energy and the electron affinity, substantially [5–8]. The situation is additionally complicated by the fact that there are actually a number of band gap values reported, all concluded from optical absorption experiments. They range from the indirect gap of 3.28 eV reported in Ref. [9] to values of 4.0 or 4.3 eV [10, 11]. The lack of experimental data may partially be related to the fact that the crystal growing process results in samples that are not stoichiometric, but Li deficient. In fact, many LN applications depend on intentional impurities of the material. Moreover, the paraelectric phase is stable in a small temperature window only.

Only few calculations, however, address the optical and electronic properties. Most *first-principles* band-structure calculations, e.g., Refs. [12, 13], are based on a single-particle picture and neglect quasiparticle effects that typically widen the band gap between occupied and empty states by a large fraction of its value [14]. The seemingly good agreement between measured and calculated band gaps for LN may therefore result from a fortuitous error cancellation between the possibly large exciton binding energy and the electronic self-energy. An early theoretical study by Ching *et al.* [15] indicates the importance of self-energy effects: Using the approximate Sterne-Inkson model [16], they predicted self-energy corrections of the order of one eV. However, the single-particle gap in Ref. [15] is much smaller (2.62 eV for the ferroelectric phase) than in the work [13] (3.69 eV). The most recent study [2] on the band structure found indirect band gaps of 3.48

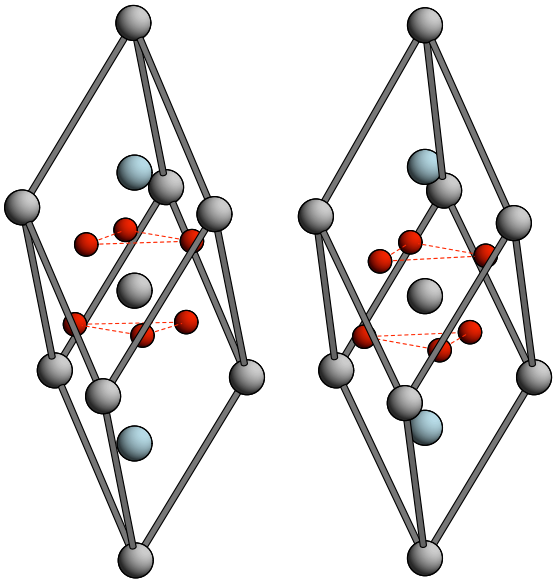

Figure 1 (color online) Primitive unit cell of the ferroelectric (left) and paraelectric phase (right) of LN. Light, small and dark balls indicate the positions of O, Li, and Nb, respectively.

and 2.47 eV for the ferro- and the paraelectric phase within the single-particle approximation. On top of this quasiparticle effects were included by using the *GW* approach [19] where a model dielectric function [20] was used as a further approximation to calculate W. With this scheme a band gap of 6.3 eV was obtained for the ferroelectric phase and 4.5 eV for the paraelectric phase respectively.

The present study aims at a more accurate calculation of the LN electronic excitation energies by replacing the model dielectric screening used in the GW calculations of Ref. [2] by a screening function calculated from *first principles*. We use density functional theory in generalized gradient approximation (DFT-GGA) to determine the structurally relaxed ground state of both the ferro- and paraelectric LN phase. The reliability of our scheme is demonstrated by comparing the structural properties with earlier theoretical data and experiment. DFT-GGA also provides the Kohn-Sham eigenvalues and eigenfunctions that enter the single- and two-particle Green's functions. The the electronic quasiparticle spectrum is obtained within the GW approximation (GWA) [19] to the exchange-correlation self-energy.

2 Methods In detail, we start from *first-principles* projector augmented wave (PAW) calculations, using the VASP implementation of the DFT-GGA [21,22]. A 4×4×4 mesh is used to sample the Brillouin zone. The mean-field effects of exchange and correlation in GGA are modeled using the PBE functional [23]. The plane-wave cutoff for the wave-function expansion is 30 Ry. We performed bulk calculations using the unit cell containing 10 atoms. The shape as well as the positions of the atoms were relaxed until the remaining forces on the atoms are below 5 meV / Å. The obtained equilibrium geometries are used in all subsequent calculations.

While the plane-wave pseudopotential approach works well for sp-bonded semiconductors and simple metals, it becomes inefficient for transition metals and rare earths, where a large number of plane waves are needed to accurately describe the localized d or f orbitals. A similar problem occurs in oxides and other compounds involving first-row elements due to the hard pseudopotentials that only contain minimal screening of the ionic core by the innermost $1s$ electrons. Therefore, these materials are best studied within an all-electron scheme that treats core and valence shells on an equal footing and already incorporates the rapid oscillations of the wave functions close to the nuclei in the basis functions themselves. So we used a full-potential linearized augmented-plane-wave (FLAPW) [24] approach to DFT, which is implemented in the FLEUR package [25] to calculate the electronic structure of LN. The FLAPW method divides space into nonoverlapping muffin-tin spheres centered at the atomic positions and into the interstitial region. The basis functions inside the muffin-tin spheres are constructed from numerical solutions of the radial Schrödinger equation with fixed energy parameters, whose products lie outside the vector space spanned by the original basis functions. Therefore, products of the original basis functions may instead be used to construct a mixed product basis [26], in which the matrix elements of the Coulomb potential with initial and final states are then accurately represented. For the muffin-tin radii we choose $r_{\mathrm{O}} = 1.74$ a.u., $r_{\mathrm{Nb}} = 1.74$ a.u. and $r_{\mathrm{Li}} = 1.94$ a.u. The plane-wave cutoff for the interstitial region is 4.3 a.u. and the Brillouin zone is sampled by a 4×4×4 $\mathbf{k}$-point mesh. Furthermore it was necessary to define one local orbital for the lithium and two local orbitals for the niobium atoms respectively.

In the second step, we include electronic self-energy effects, i.e., replace the GGA exchange and correlation potential by the nonlocal and energy-dependent self-energy operator $\Sigma(\mathbf{r}, \mathbf{r}'; E)$. We calculate Σ in the GW approximation (GWA) [17–19], from the convolution of the single-particle green function G and the dynamically screened Coulomb interaction W.

A full quasiparticle calculation in the *GW* approximation involves several difficulties such as the calculation of the frequency-dependent dielectric function and the solution of a Schrödinger-like equation with a nonlocal and energy dependent self-energy operator which is non-Hermitian as opposed to the case of most eigenvalue problems involving a local energy independent potential. On top of these difficulties the calculations should actually be carried out self-consistently meaning that the output quasiparticle wave functions and energies should be used in calculating the self-energy operator from which the results are obtained.

Performing a self-consistent *GW* calculation is a heavy undertaking. It is well known that a non-self-consistent calculation, i.e., approximating *GW* by G_0W_0, where the screening W_0 is taken from the random-phase approximation (RPA), gives reasonable results. Therefore this approximation-scheme was used. Due to the size of the supercell a 2×2×2 sampling of the Brillouin zone is reasonable.

3 Results and discussion The relaxed ground-state geometries for ferro- and paraelectric LN are the starting points for all further investigations. In paraelectric LN, the Li and Nb atoms are at Wyckoff positions 6a and 6b (hexagonal axes), respectively, while the O atoms are located at 18e, with internal parameter x. We determine lattice constants $a = 5.219$ Å, $c = 13.756$ Å, and $x = 0.041$. The measured values amount to 5.289 Å, 13.848 Å, and $x = 0.06$ [27]. The usage of GGA often leads to a slight overestimation of lattice constants. The fact that an underestimation of about 1% occurs here may be related to the thermal expansion of the sample – the paralelectric phase is stable for temperatures above 1480 K – which is not included in our ground-state calculations. Earlier GGA results [12] are in fact quite similar to our findings: $a = 5.255$ Å, $c = 13.791$ Å, and $x = 0.048$.

In ferroelectric LN, Li and Nb are located at Wyckoff position 6a (hexagonal axes) with internal parameter z_{Nb}; oxygen atoms are at 18b with parameters u, v, and w. Following the notation in Ref. [12], we determine $a = 5.161$ Å, $c = 13.901$ Å, $z_{Nb} = 0.0339, u = 0.01205, v = 0.0278$, and $w = 0.0191$. The deviation from experiment [27] ($a = 5.151$ Å, $c = 13.876$ Å, $z_{Nb} = 0.0329, u = 0.00947, v = 0.0383, w = 0.0192$) is much smaller than for the paraelectric phase, corroborating our assumption that thermal expansion may be responsible for much of the deviation in the paraelectric case. Again, close agreement with the GGA results of Veithen and Ghosez is observed [12].

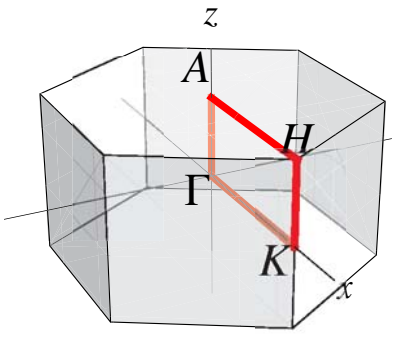

Figure 2 (color online) Notation of high symmetry Brillouin zone points used in the present work.

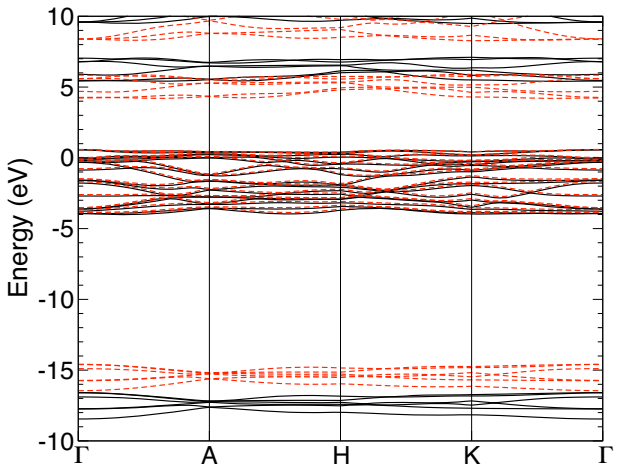

Figure 3 (Color online) Calculated band structures of ferroelectric LN right calculated within the DFT-GGA (dashed lines) and the GW approximation (solid lines).

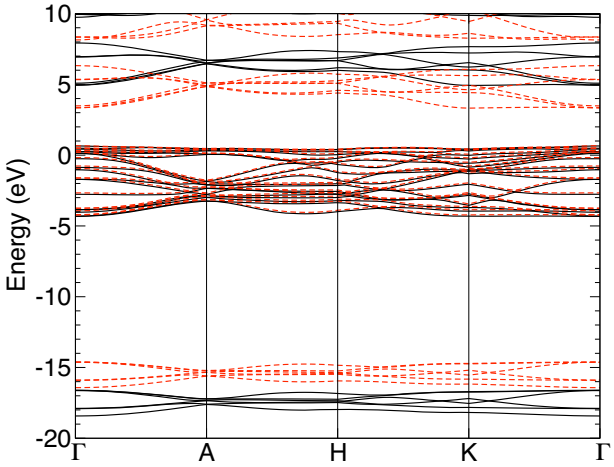

Figure 4 (Color online) Calculated band structures of paraelectric LN right calculated within the DFT-GGA (dashed lines) and the GW approximation (solid lines).

The results above indicate good agreement between the DFT-GGA calculations and experiment concerning the structural ground state properties of LN. On this basis we can start to analyze the electronic properties. In Fig. 3 and 4 we plot the Kohn-Sham energies along high symmetry lines of the hexagonal Brillouin zone (cf. Fig. 2) of ferro- and paraelectric LN. Within the single-particle approximation, the ferro- and paraelectric phases have indirect band gaps of 3.61 and 2.57 eV, respectively. These values agree well with other recent DFT calculations [2], which predict 3.48 and 2.52 eV, respectively. The valence-band maximum (VBM) occurs at the Γ point for both phases,

while the conduction-band minima (CBM) are located at 0.4 $\Gamma - K$ and the K point for the ferro- and paraelectric phase, respectively.

The single-particle excitations are accompanied by the rearrangement of the remaining electrons in the solid, that screen the excited electrons (above the Fermi level) and excited holes (missing electrons below the Fermi level). Polar materials like LN, however, feature longitudinal optical phonons that give rise to macroscopic electric fields that couple to the excited electrons and holes and modify their motion. It can be expected that the lattice polarizability contributes to the dressing of the quasiparticles. This effect is not included in the GWA band structures shown in Fig. 3 and 4, that rest on the assumption of a pure electronic screening. To study the effect of the lattice polarizability on the single-particle excitation energies, in principle the electron-phonon coupling needs to be considered which is part of our future investigations.

Method	paraelectric	ferroelectric
DFT (FLAPW)	2.57	3.61
DFT (plane wave) [2]	2.48	3.47
GW (FLAPW)	4.21	4.71
GW (plane wave) [2]	5.37	6.53
Exp. [1]	-	3.78

Table 1 Comparison of band gap energies (eV) for the para- and the ferroelectric phase of LN.

Thus the band gap of ferroelectric LN is calculated to be 4.71 eV, while we obtain 4.21 eV for paraelectric LN. A comparison with earlier *GW* calculations [2] where a model dielectric model function was used, we observe that our results for the band gap are significantly smaller. However, the present work nevertheless corroborates the finding of Ref. [2] that the LN band gap is indeed substantially larger than the value frequently cited in the literature.

Acknowledgements The calculations were performed using grants of computer time from the Paderborn Center for Parallel Computing (PC^2) and the Höchstleistungs-Rechenzentrum Stuttgart. Financial support by the DFG is acknowledged.

References

[1] A. Dhar and A. Mansing, J. Appl. Phys. **68**, 5804 (1990)
[2] W.G. Schmidt, M. Albrecht, S. Wippermann, S. Blankenburg, E. Rauls, F. Fuchs, C. Rödl, J. Furthmüller, and A. Hermann, Phys. Rev. B **77**, 035106 (2006).
[3] C. Friedrich, A. Schindlmayr, S. Blügel, and T. Kotani, Phys. Rev. B **74**, 045104 (2006).
[4] A. Dhar and A. Mansingh, J. Appl. Phys. **68**, 5804 (1990).
[5] S. Albrecht, L. Reining, R. Del Sole, and G. Onida, Phys. Rev. Lett. **80**, 4510 (1998).
[6] L. X. Benedict, E. L. Shirley, and R. B. Bohn, Phys. Rev. Lett. **80**, 4514 (1998).
[7] M. Rohlfing and S. G. Louie, Phys. Rev. Lett. **83**, 856 (1999).
[8] P. H. Hahn, W. G. Schmidt, K. Seino, M. Preuss, F. Bechstedt, and J. Bernholc, Phys. Rev. Lett. **94**, 037404 (2005).
[9] Z. Jiangou, Z. Shipin, X. Dingquan, W. Xiu, and X. Guanfeng, J. Phys.: Condens. Matter **4**, 2977 (1992).
[10] D. Redfield and W. J. Burke, J. Appl. Phys. **45**, 4566 (1974).
[11] S. Kase and K. Ohi, Ferroelectrics **8**, 419 (1974).
[12] M. Veithen and P. Ghosez, Phys. Rev. B **65**, 214302 (2002).
[13] I. V. Kityk, M. Makowska-Janusik, M. D. Fontana, M. Aillerie, and F. Abdi, J. Appl. Phys. **90**, 5542 (2001).
[14] F. Bechstedt, in: Festköperprobleme/ dvances in Solid State Physics, edited by U. Rössler (Vieweg, Braunschweig/Wiesbaden, 1992), Vol. 32, p. 161.
[15] W. Y. Ching, Z.-Q. Gu, and Y.-N. Xu, Phys. Rev. B **50**, 1992 (1994).
[16] S. J. Jenkins, G. P. Srivastava, and J. C. Inkson, Phys. Rev. B **48**, 4388 (1993).
[17] L. Hedin, Phys. Rev. **139**, A796 (1965).
[18] L. Hedin and S. Lunquist, in: Solid State Physics, edited by F. Seitz, D. Turnbull, and H. Ehrenreich (Academic, New York, 1969), Vol. 23, p. 1.
[19] M. S. Hybertsen and S. G. Louie, Phys. Rev. B **34**, 5390 (1986).
[20] F. Bechstedt, R. Del Sole, G. Cappellini, and L. Reining, Solid State Commun. **84**, 765 (1992).
[21] G. Kresse and J. Furthmüller, Comput. Mat. Sci. **6**, 15 (1996).
[22] G. Kresse and D. Joubert, Phys. Rev. B **59**, 1758 (1999).
[23] J. Perdew, K. Burke, and M. Ernzerhof, Phys. Rev. Lett. **77**, 3865 (1996).
[24] D.J. Singh, Planewaves, Pseudopotentials and the LAPW Method (Kluwer, Dordrecht, 1994).
[25] see `http://www.flapw.de`
[26] T. Kotani and M. van Schilfgaarde, Solid State Commun. **121**, 461 (2002).
[27] H. Boysen and F. Altorfer, Acta Crystallogr., Sect. B: Struct. Sci. **50**, 405 (1994).